Discovery of small molecule inhibitors targeting the SUMO-SIM interaction using a protein interface consensus approach

Electronic Supplementary Information

Arnout R.D. Voet,[‡a] Akihiro Ito,[‡bc] Mikako Hirohama,[be] Seiji Matsuoka,[d] Naoya Tochio,[§f] Takanori Kigawa,[f] Minoru Yoshida[bcde] and Kam Y.J. Zhang[*a]

[a] Zhang Initiative Research Unit, RIKEN, 2-1 Hirosawa, Wako, Saitama 351-0198, Japan. E-mail: kamzhang@riken.jp

[b] Chemical Genetics Laboratory, RIKEN, 2-1 Hirosawa, Wako, Saitama 351-0198, Japan.

[c] Chemical Genomics Research Group, RIKEN Center for Sustainable Resource Science, 2-1 Hirosawa, Wako, Saitama 351-0198, Japan.

[d] Drug Discovery Platforms Cooperation Division, RIKEN Center for Sustainable Resource Science, 2-1 Hirosawa, Wako, Saitama 351-0198, Japan.

[e] Japan Science and Technology Corporation, CREST Research Project, 4-1-8 Honcho, Kawaguchi, Saitama 332-0012, Japan.

[f] Laboratory for Biomolecular Structure and Dynamics, Quantitative Biology Center, RIKEN, 1-7-22 Suehiro, Yokohama, Kanagawa 230-0045, Japan.

[‡] These authors contributed equally to this work.

[§] Current Address: Department of Mathematical and Life Sciences, Graduate School of Science, Hiroshima University, 1-3-1 Kagamiyama, Hiroshima 739-8530, Japan.

Virtual screening protocol

Druggability analysis of the SUMO structure was performed using the HotPatch server[1], indicating an absence of a clear small molecule binding cleft, however a small hydrophobic trench is present. Electrostatic analysis of the SUMO-SIM interface was performed using APBS.[2]

The compound database (Namiki Shoji CO., LTD, Tokyo, Japan) used for virtual screening was prepared by enumerating the different stereo and tautomers using OpenEye's Quacpac and Flipper tools (OpenEye, Santa Fe, NM, USA). A maximum of 250 conformations for each unique molecule was generated using OpenEye's Omega2 tool.[3, 4] Using the Filter tool, molecules with a net positive charge or more hydrogen bond donors than acceptors were removed.

The consensus pharmacophore was created using MOE (Molecular Operating Environment, Chemical Computing Group, Montreal, Canada) pharmacophore implementation with the "PCHD scheme", based on SUMO-SIM interactions observed in the following PDBs: 1WM3, 1WYW, 1Z5S, 2ASQ, 2KQS, 3KYC and 3RD2. First the structures were superposed on the backbone of the SUMO proteins, and then the consensus interactions were computed for the SUMO interacting amino acids (and water molecules). The final pharmacophore query consisted of 3 "hydrophobic or aromatic" features (representing hydrophobic side chain interactions) and 2 hydrogen bond donor and 2 hydrogen bond acceptor features (including directionality of the interaction) that resemble the main chain interactions at the SUMO interface (supplementary Figure 1). As a forbidden volume, the union of the side chain conformations of PDB 1WYW and 1Z5S was chosen. During virtual screening using the pharmacophore query, a partial match was allowed, while the 3 hydrophobic/aromatic features and the 2 central hydrogen bonds were essential, it was sufficient to hit only one out of the 2 "outside" hydrogen bond features.
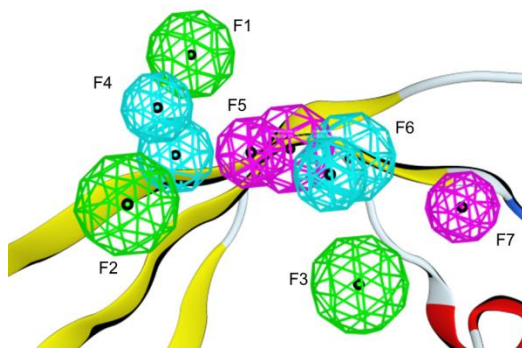

Figure S1: Graphical depiction of the pharmacophore query representing the key interactions at the SUMO-SIM interface. The hydrophobic/aromatic features (F1, F2 and F3) are presented as green spheres. The hydrogen bonds are represented as magenta or blue spheres for hydrogen bond acceptors or donors respectively. During the pharmacophore search, partial matching was allowed and it was sufficient to hit only one of the non-essential features F4 and F7.

After the pharmacophore query, the remaining compounds were docked using GOLD in virtual screening default settings[5], with the PLP scoring function[6], and for 10 runs per compound, to the 2 different receptor conformations. The docked conformations were rescored using DrugScoreX[7, 8]. Compounds that ranked in the 2 different receptors for the 2 different scoring functions in the lowest 50 percent were removed. The remaining compound binding modes were post-filtered using the pharmacophore query to remove undesired binding modes. Finally the compound binding modes were compared between the 2 different docking receptors and the compounds were retained only if the RMSD of the two binding modes for each compound was within 0.5 Å (absolute positions). In a subsequent step, the remaining binding modes were filtered using EleKit[9] for electrostatic similarity with the SIM DAXX peptide, removing all docked compounds without similarity. Finally the remaining compounds were selected after visual inspection of the binding mode to the different receptor conformations with the DrugScoreX[7, 8] visualization script for Pymol (Schrödinger LCC). Up to 3 derivatives belonging to the same chemotype were allowed to be selected.

After the first round, derivatives of the most promising active compounds (SSI-012, SSI-020, SSI-038 and SSI-062 belong to one chemical class, while SSI-041 and SSI-060 belong to other classes) were identified by similarity searching using MACCS and 3 point pharmacophore fingerprints using MOE.
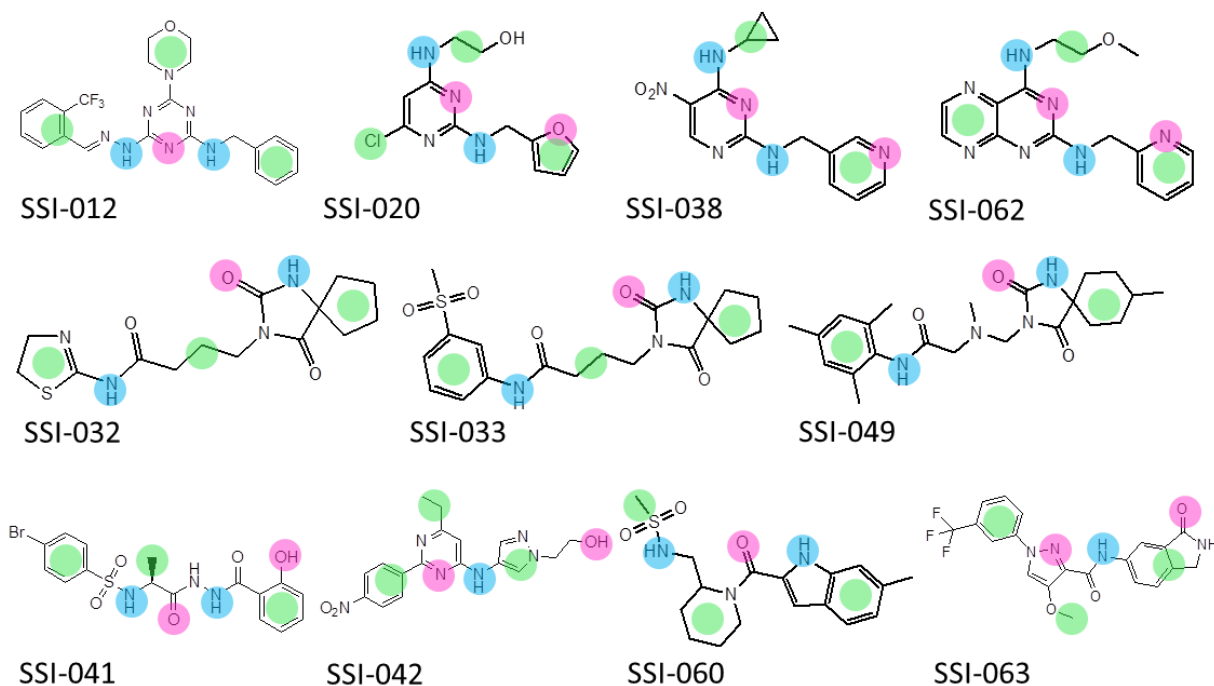
Figure S2: The first hit molecules oriented according to the pharmacophore query represented in supplementary Figure S1. Green spheres indicate the mapping of the hydrophobic/aromatic pharmacophore features, blue and magenta of the hydrogen bond donor/acceptor features respectively.

Bacterial protein expression and purification

Recombinant His-tagged SUMO1 protein was purified as described[10] with minor modifications. Briefly, the pET-based bacterial expression plasmids containing SUMO1 cDNA were introduced into Escherichia coli BL21 (DE3). The expression of recombinant proteins was induced by addition of 0.3 mM isopropyl-b-D-galactopyranoside (IPTG) for 8 h. Purification of His-tagged SUMO1 proteins were carried out using (Ni^{2+})-affinity column (QIAGEN). The SUMO2/3 isoform protein was purified similarly.

AlphaLISA assay

His- tagged SUMO1 (3 µM) and biotinylated DAXX-SIM peptide were incubated in 10 µl of a reaction buffer containing 20 mM HEPES (pH 7.5), 150 mM KCl, and 0.05% Tween20 at room temperature for 1 h. Then, nickel chelate acceptor beads and streptavidin-coated donor beads (20 µg/ml each) were sequentially added into the reaction and incubated in the dark at room temperature for additional 30 min, respectively. The signal was measured using an EnSpire[TM] (PerkinElmer).[11]
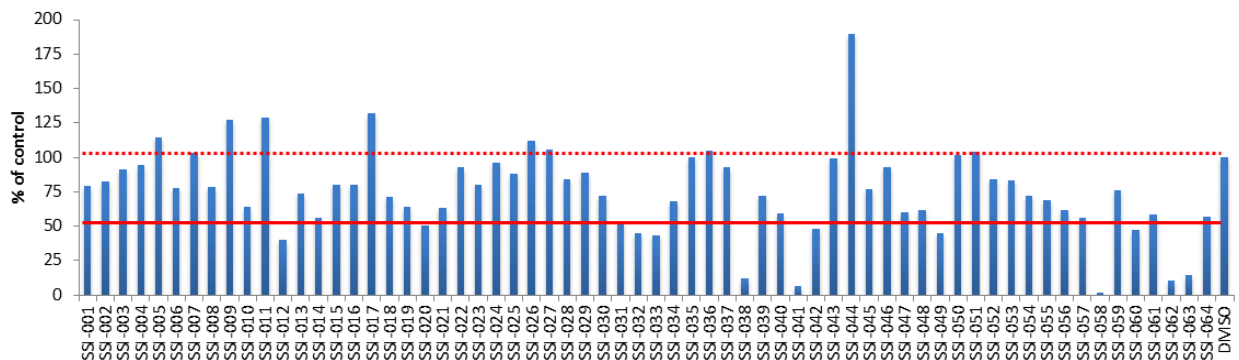
Figure S3: AlphaLISA results of the first round of compounds at 500µM concentration. The dotted and solid red lines indicate the 100% effect and 50% effect relative DMSO respectively.
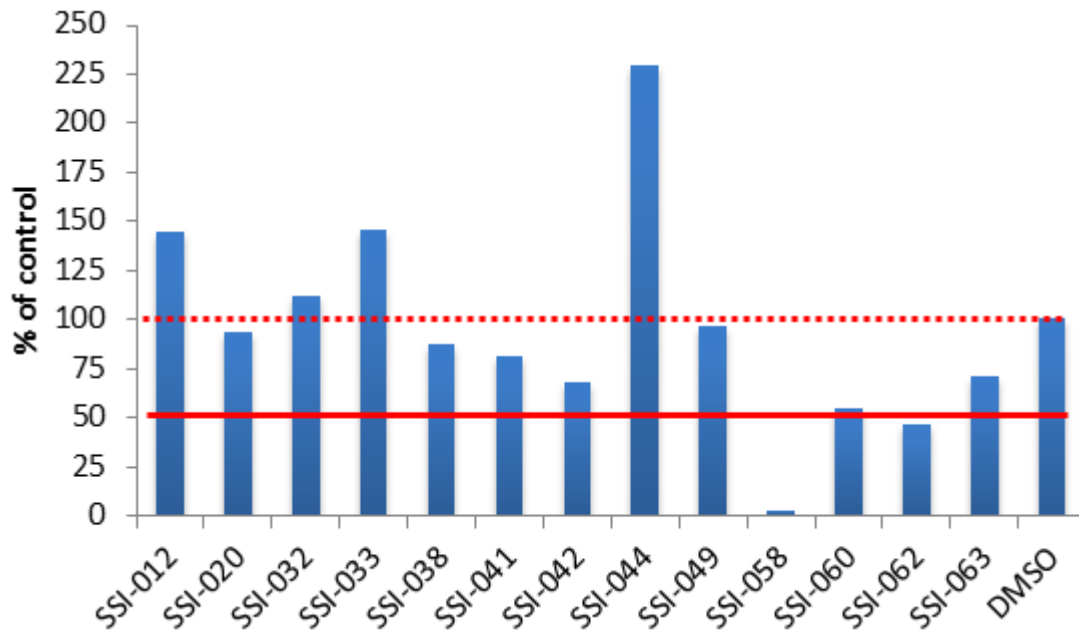
Figure S4: AlphaLISA results of the first round 500 μM hit compounds at 100μM compound concentration. The dotted and solid red lines indicate the 100% effect and 50% effect relative DMSO respectively.
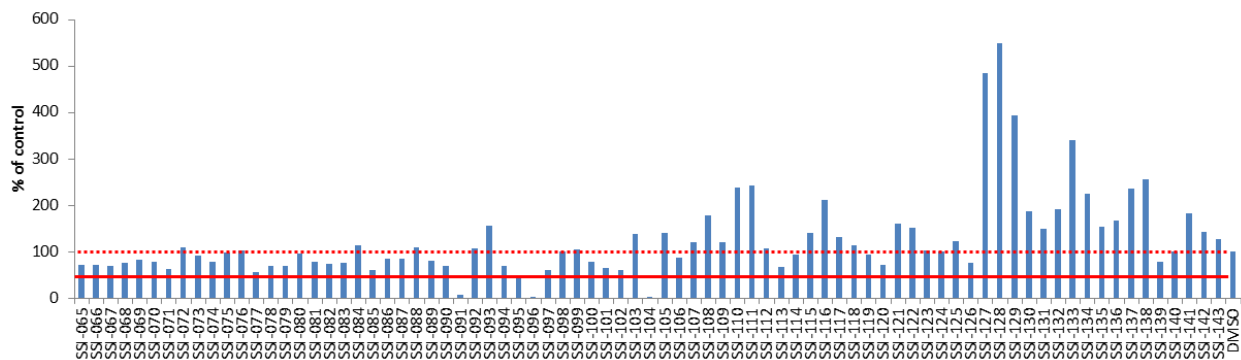
Figure S5: AlphaLISA results of the second round of compounds at 100μM concentration. The dotted and full red lines indicate the 100% effect and 50% effect relative DMSO respectively.
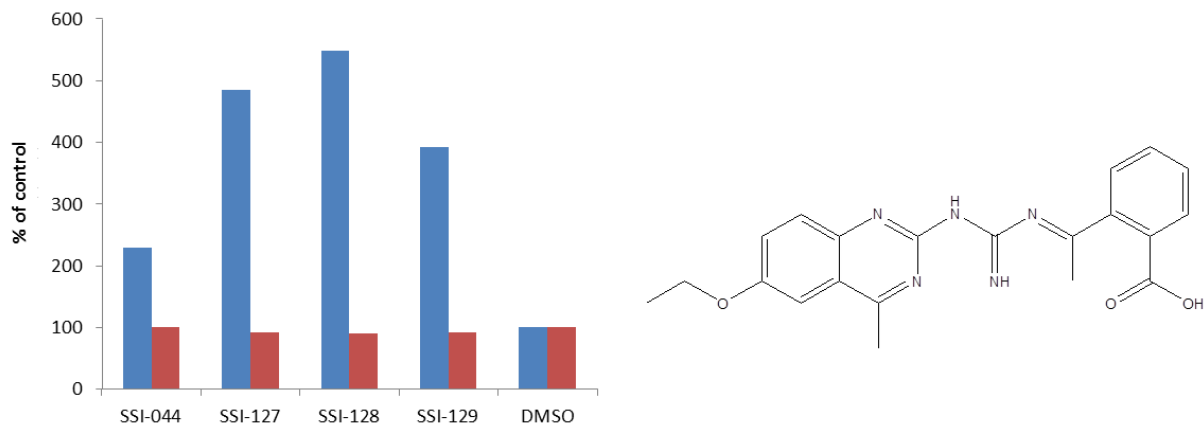
Figure S6: AlphaLISA results the SUMO-SIM interaction stimulators at 100µM compound concentration (blue) with the TruHits screen (red) indicating the stimulatory effect is not an artifact inherent to the compound structures. All chemical structures are derivatives of the same chemotype. On the right the chemical structure of the strongest stimulators SSI-128 is depicted.
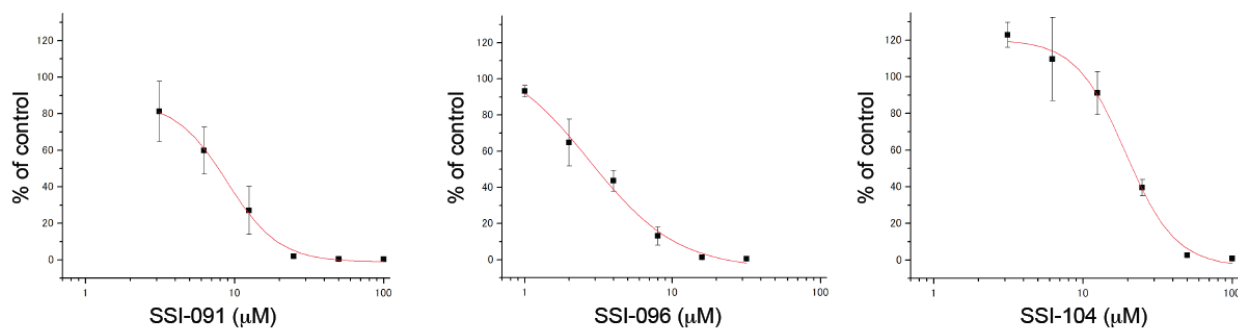
Figure S7: Dose response curves of the most potent compounds.

SPR binding Analysis

The SPR experiment was performed with a Biacore T200 (GE Healthcare). His-SUMO1 (or His-SUMO2/3) (0.46 µg/ml) in running buffer (HBS-P+, GE Healthcare) was immobilized to approximately 280 RU on a Series S Sensor Chip NTA (GE Healthcare) using a standard ligand capture method with a His Capture Kit (GE Healthcare). A flow cell without immobilized proteins was used as reference. The analyte solution was prepared by a serial dilution of compounds with the running buffer containing 5% DMSO. Binding analysis was conducted at a flow rate of 30 µl/min at 25°C. In each run, the association phase and the following dissociation phase were monitored for 60 and 120 seconds, respectively. Blank control run was performed by the injection of running buffer containing 5% DMSO. From the obtained reference-subtracted

sensorgrams, the dissociation constant (K_D) of compounds was estimated by a global fitting to a simple 1:1 binding model in the Biacore evaluation software (GE Healthcare). The sensorgrams were corrected for DMSO bulk response by using calibration curves obtained with running buffer containing 4-6% DMSO.
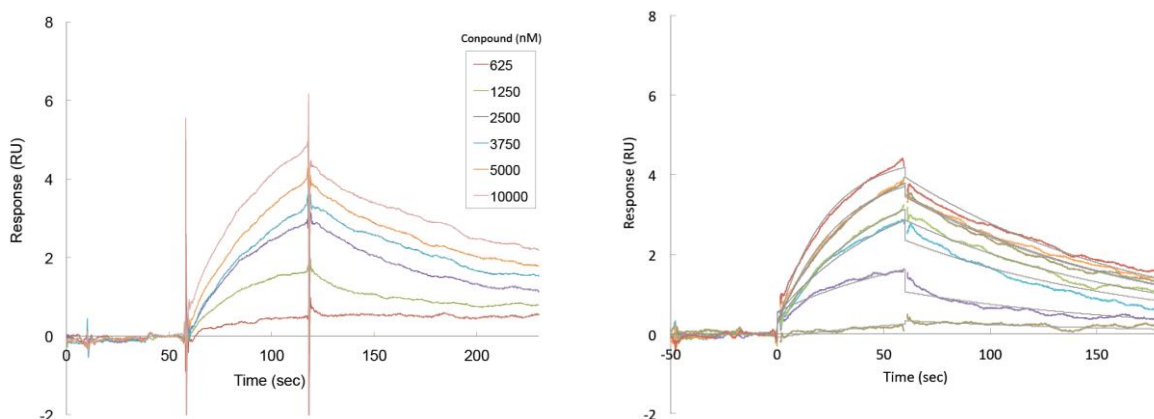
Figure S8: SPR sensorgrams of SSI-091 binding to immobilized SUMO1 (left). The sensorgrams were fitted to a 1:1 binding model by an analysis using the Biacore evaluation software (GE Healthcare) (right).

Table S1: Kinetic parameters of most potent compounds in SPR experiments

ID-number	Kon (M/S)		Koff (1/S)	
	SUMO-1	SUMO-2/3	SUMO-1	SUMO-2/3
SSI-091	3.6×10^3	4.0×10^3	6.4×10^{-3}	7.1×10^{-3}
SSI-096	1.5×10^3	1.0×10^3	6.9×10^{-2}	6.0×10^{-2}
SSI-104	5.2×10^2	1.3×10^3	1.8×10^{-2}	4.2×10^{-2}

Cellular split luciferase assay

The cellular split luciferase assay was performed using two mammalian expression constructs consisting of the N-terminal fragment of *Renilla* luciferase fused to SUMO1 and the C-terminal fragment of *Renilla* luciferase fused to the SIM sequence from the Daxx protein, respectively. 293T cells were transfected with the two above expression vetors, followed by treatment with inhibitors for 24 h. After cells were lysed in passive lysis buffer, the bioluminescence generated by adding coelenterazine into the cell lysates was measured using a luminometer.

Evaluated compounds

All evaluated compounds were purchased from Enamine or Vitas-M Laboratory through Namiki Shoji CO., LTD (Tokyo, Japan). A complete list of compounds with their activity and identity is shown at the end of this document

NMR experiments

All NMR spectra were recorded at 298 K on a 700 MHz Bruker Avance spectrometer equipped with CryoProbe.

The STD experiments were performed using non-labeled SUMO1 protein, purified as described above. The 1D ^{1}H NMR spectrum of 500 µM SSI-091 was measured in the presence of 12.3 µM non-labeled SUMO1 in 20 mM d_{18}-HEPES (pH7.5), 150 mM KCl, 5% d_6-DMSO, and 95% D$_2$O. The double off-resonance spectra were obtained when the mixture of SSI-091 and SUMO1 was irradiated at 40 ppm. The STD spectra were obtained by subtraction of the on-resonance spectrum (at 0.07 ppm) from the off-resonance spectrum (at 40 ppm).
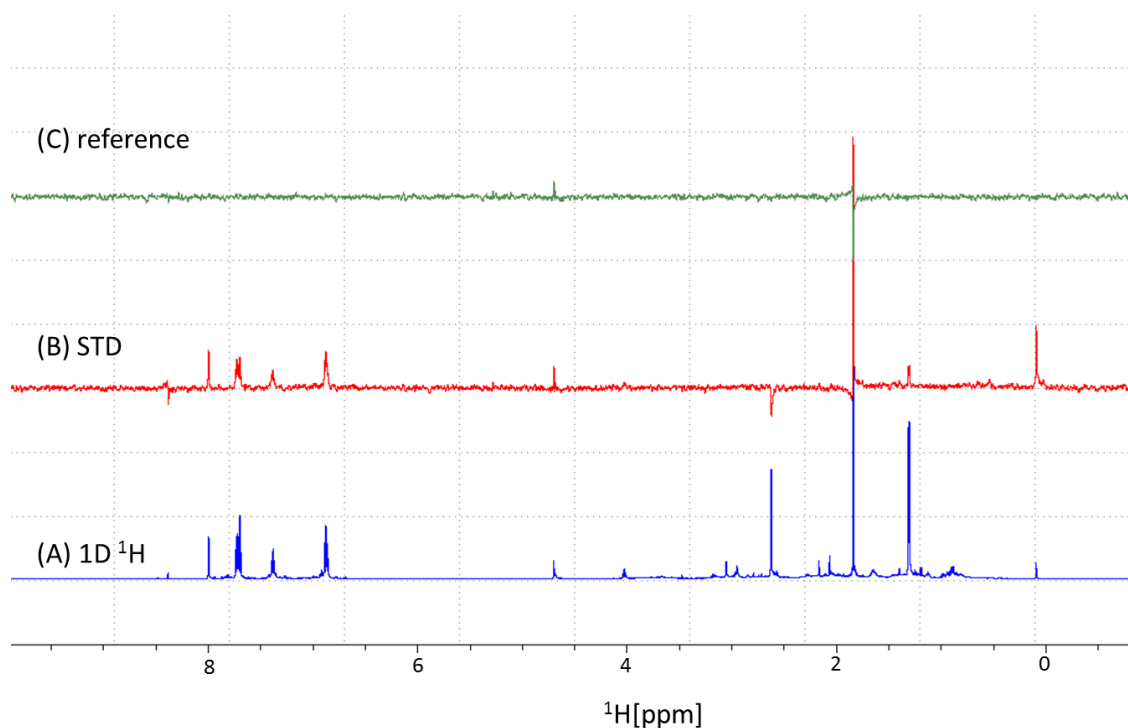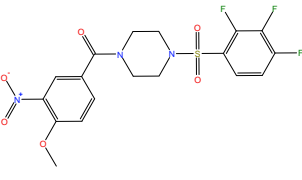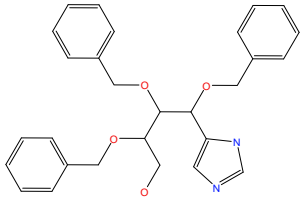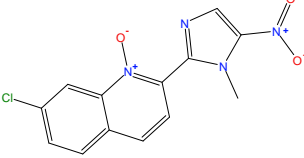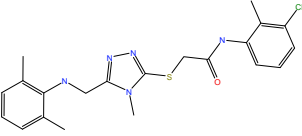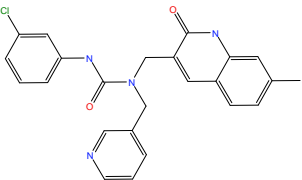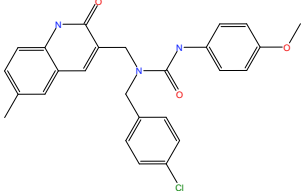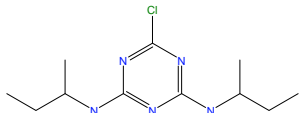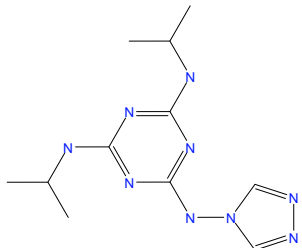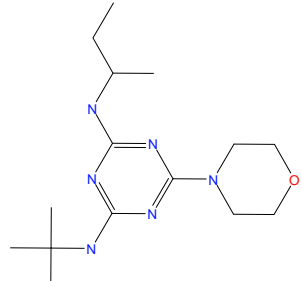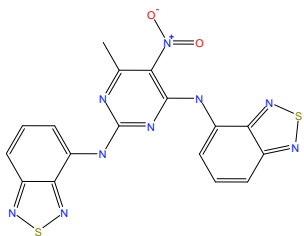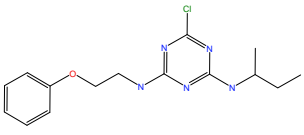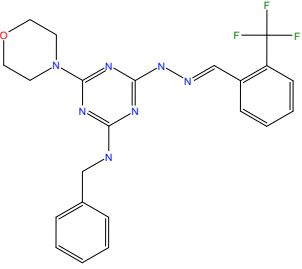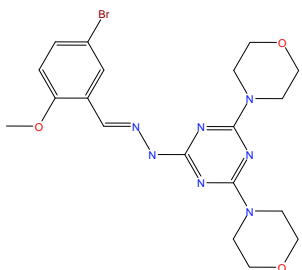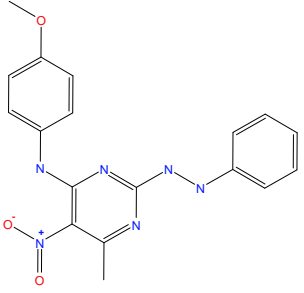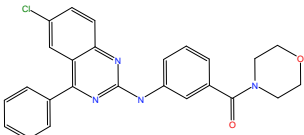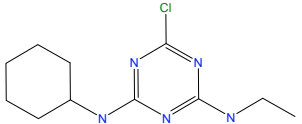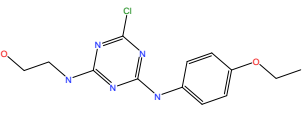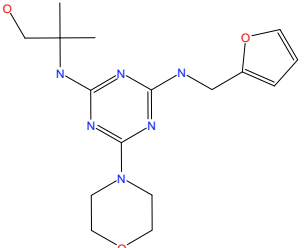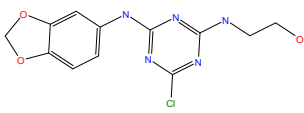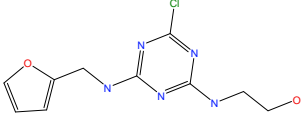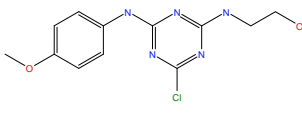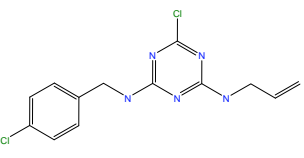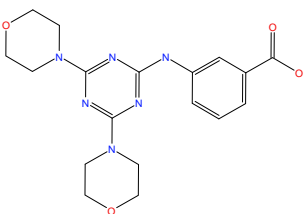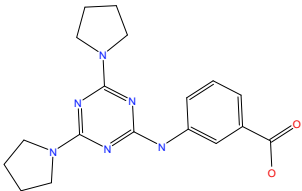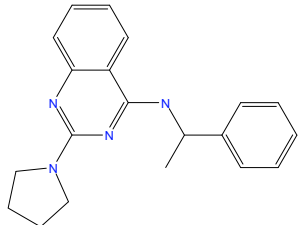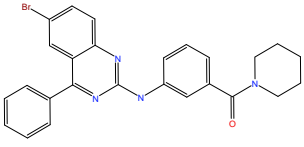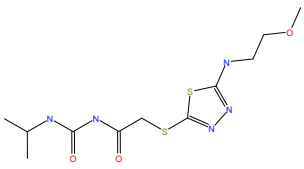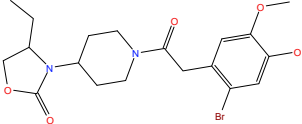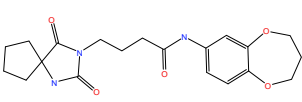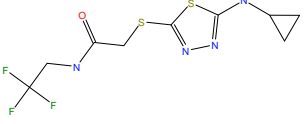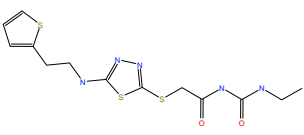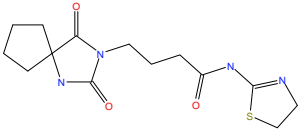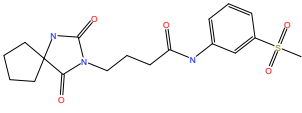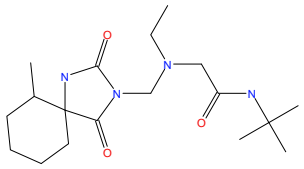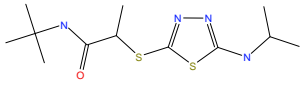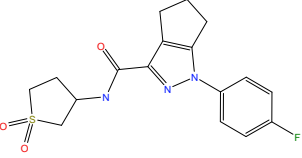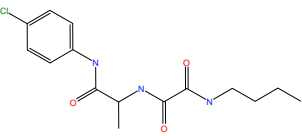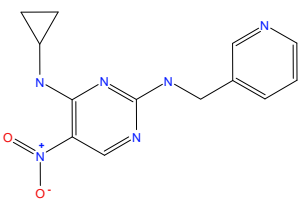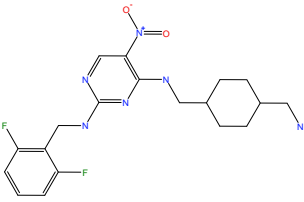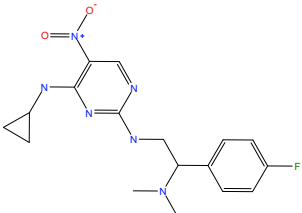
Figure S9: STD experiment for SSI-091.
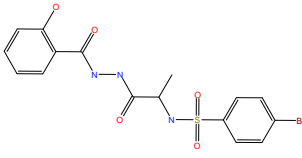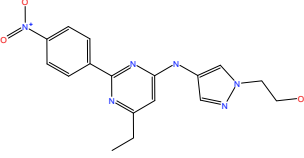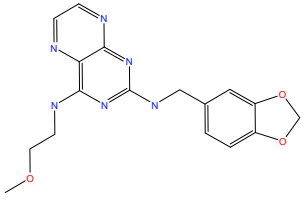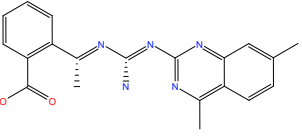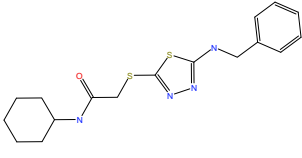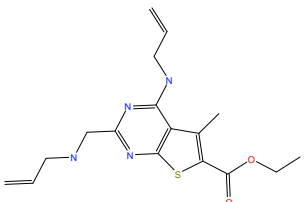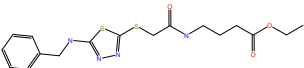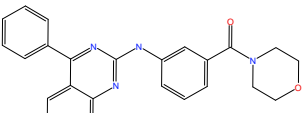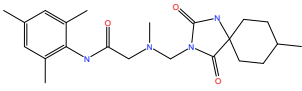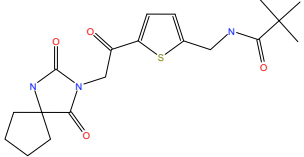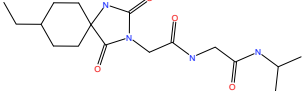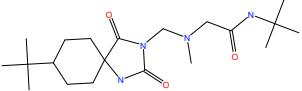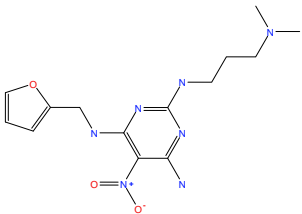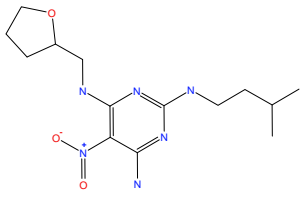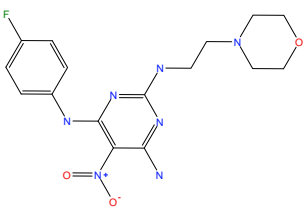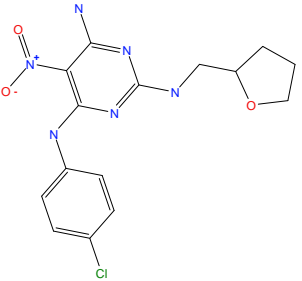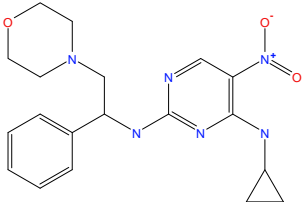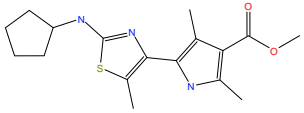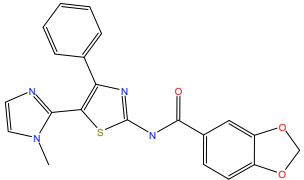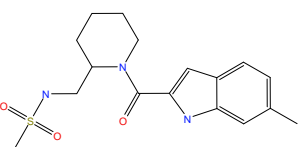
(A) 1D ^{1}H NMR spectrum of SSI-091 in the presence non-labeled SUMO1. (B) The STD spectra obtained by subtraction of the on-resonance spectrum (at 0.07 ppm) from the off-resonance spectrum (at 40 ppm). (C) The double off-resonance spectra of the mixture of SSI-091 and SUMO1.
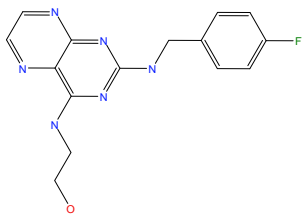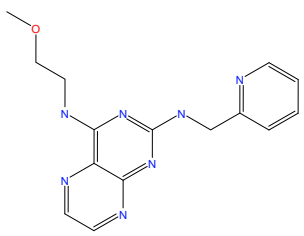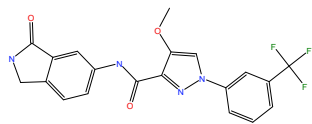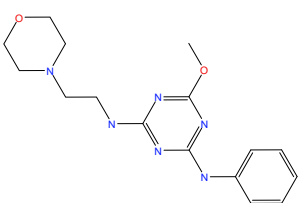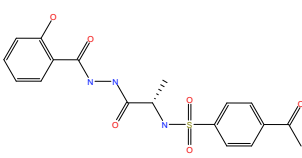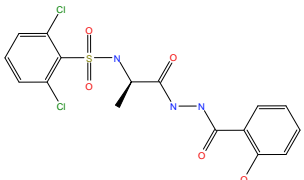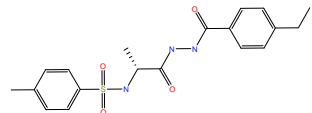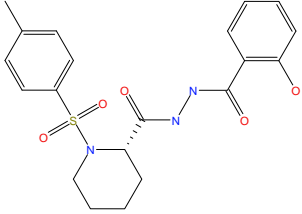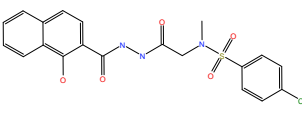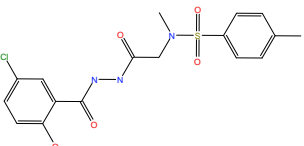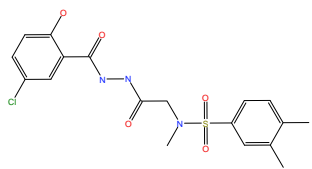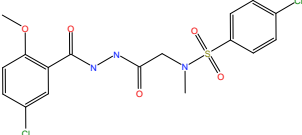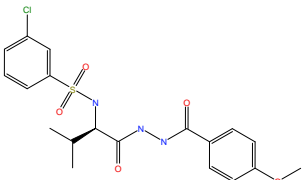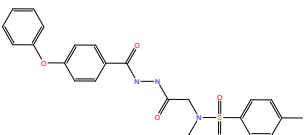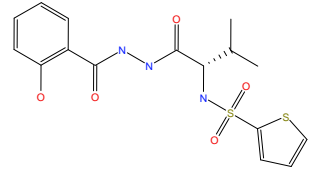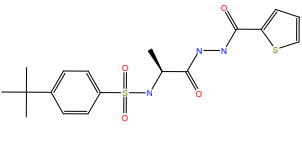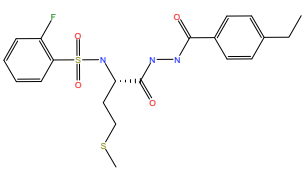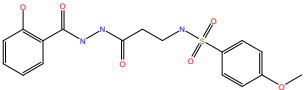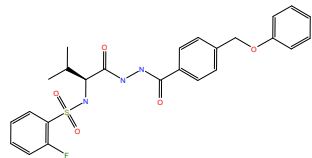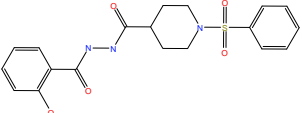
The HSQC experiments were performed using ^{13}C, ^{15}N labeled SUMO1, produced in a cell-free expression system.[12-14] The backbone chemical shift assignments of SUMO1 were accomplished by using conventional 3D triple resonance spectra at concentration of about 1 mM SUMO1. All spectra were processed using NMRPipe[15], and the programs Kujira[16] and NMRView[17] were employed for optimal visualization and spectral analyses. To experimentally map the binding interface, the ^{1}H,^{15}N HSQC spectra were measured using 50 μM ^{13}C,^{15}N labeled SUMO1 (apo spectra) and 50 μM ^{13}C,^{15}N labeled SUMO1 with 500 μM SSI-091 in 20 mM d_{18}-HEPES (pH7.5), 150 mM KCl, 5% d_{6}-DMSO (holospectrum).
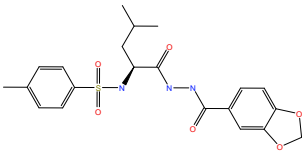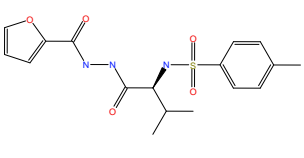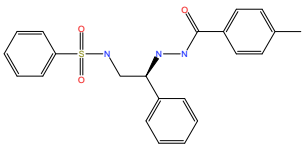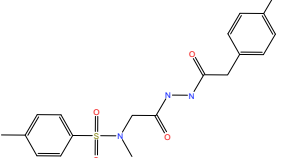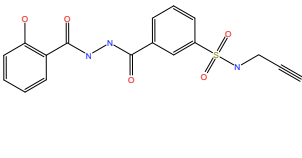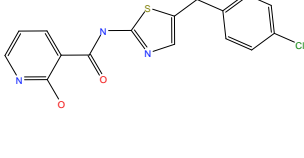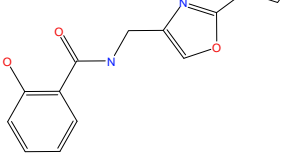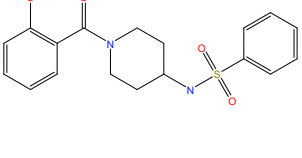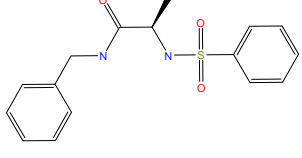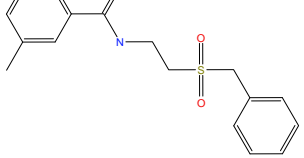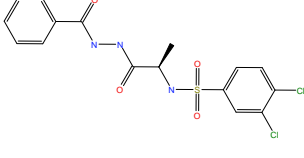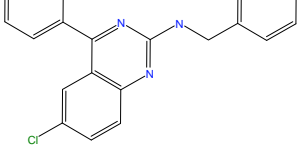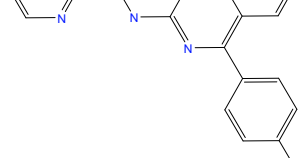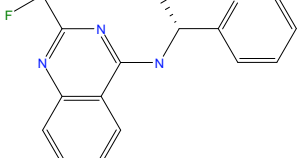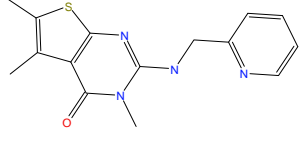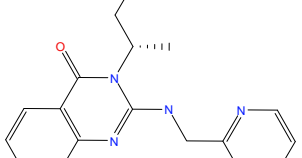
Table S2: List of structures of all evaluated compounds with percentage of inhibition measured by AlphaLisa
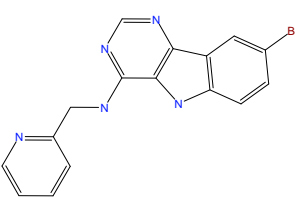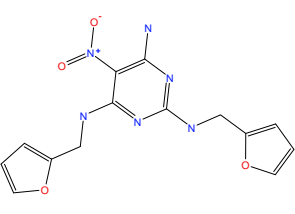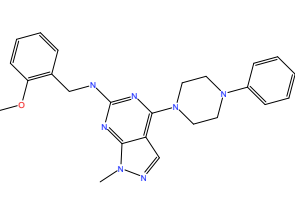
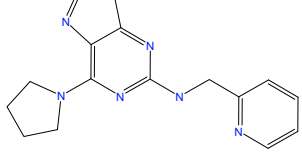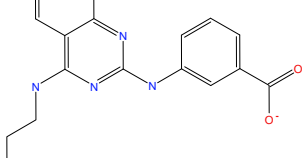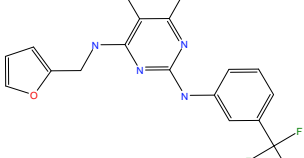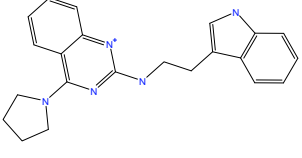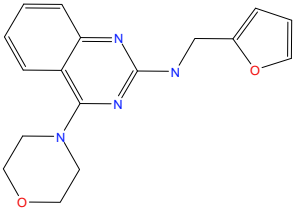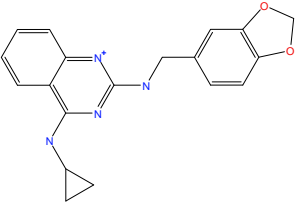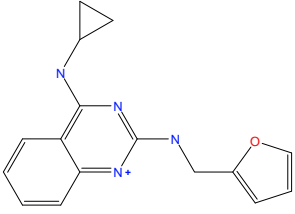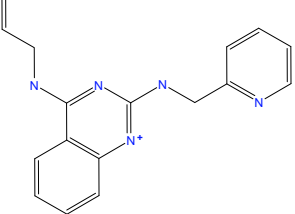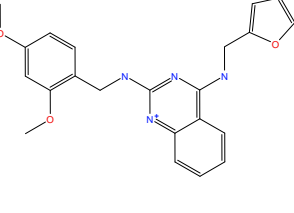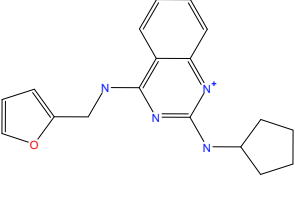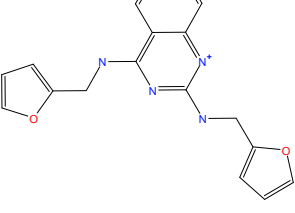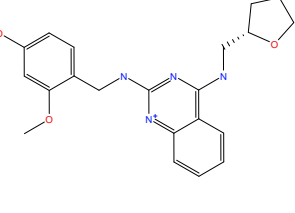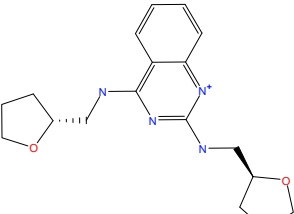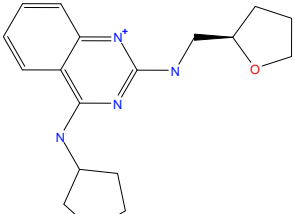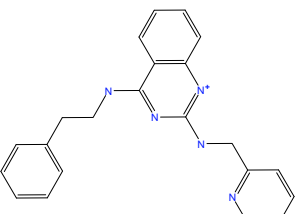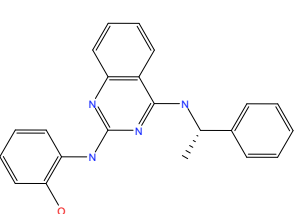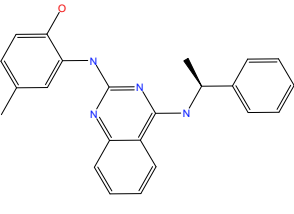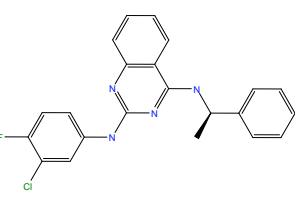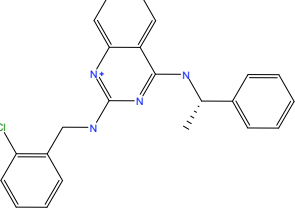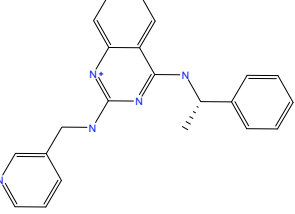|			
SSI-001 inhibition (%): 78.70	SSI-002 inhibition (%): 82.30	SSI-003 inhibition (%): 90.60	SSI-004 inhibition (%): 94.00
SSI-005 inhibition (%): 114.00	SSI-006 inhibition (%): 77.60	SSI-007 inhibition (%): 102.60	SSI-008 inhibition (%): 78.00
SSI-009 inhibition (%): 126.70	SSI-010 inhibition (%): 63.30	SSI-011 inhibition (%): 128.20	SSI-012 inhibition (%): 39.70
SSI-013 inhibition (%): 73.40	SSI-014 inhibition (%): 56.00	SSI-015 inhibition (%): 79.70	SSI-016 inhibition (%): 79.70
SSI-017 inhibition (%): 131.30	SSI-018 inhibition (%): 70.90	SSI-019 inhibition (%): 63.90	SSI-020 inhibition (%): 50.40
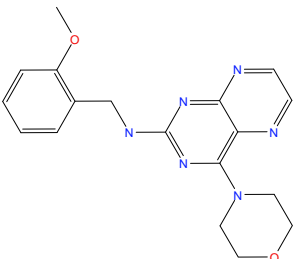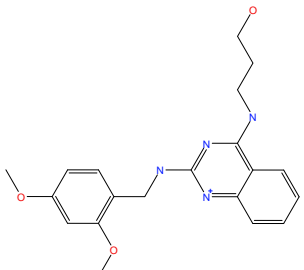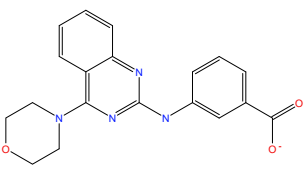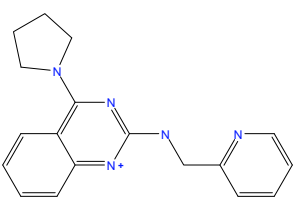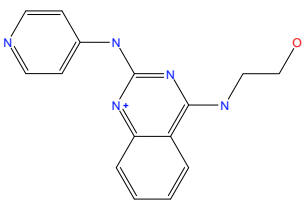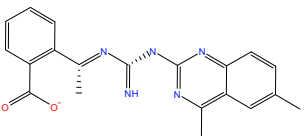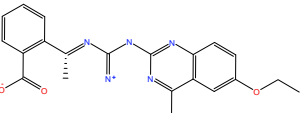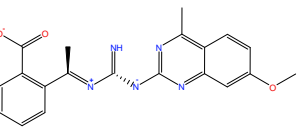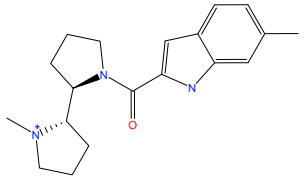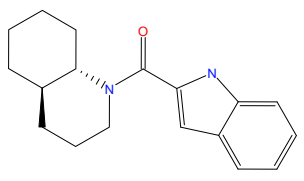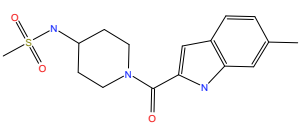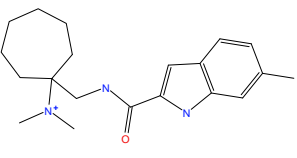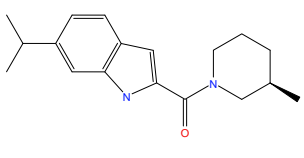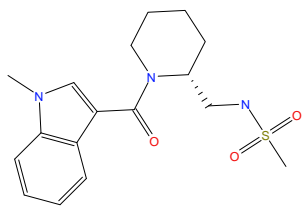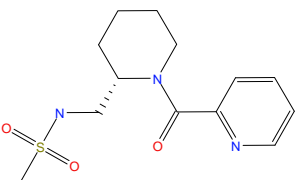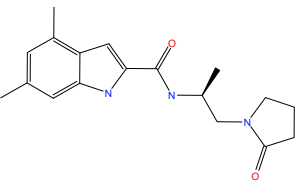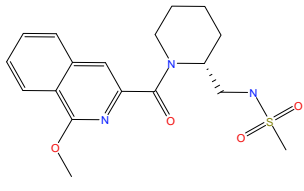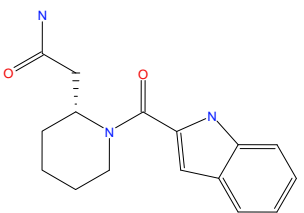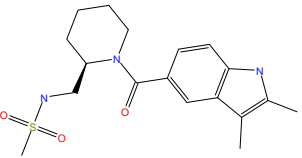
SSI-021 inhibition (%): 62.70	SSI-022 inhibition (%): 92.20	SSI-023 inhibition (%): 79.50	SSI-024 inhibition (%): 96.10
SSI-025 inhibition (%): 87.50	SSI-026 inhibition (%): 111.70	SSI-027 inhibition (%): 105.20	SSI-028 inhibition (%): 83.90
SSI-029 inhibition (%): 88.40	SSI-030 inhibition (%): 71.70	SSI-031 inhibition (%): 53.00	SSI-032 inhibition (%): 44.20
SSI-033 inhibition (%): 42.80	SSI-034 inhibition (%): 67.60	SSI-035 inhibition (%): 100.00	SSI-036 inhibition (%): 104.40
SSI-037 inhibition (%): 92.20	SSI-038 inhibition (%): 11.60	SSI-039 inhibition (%): 72.10	SSI-040 inhibition (%): 58.60

SSI-041 inhibition (%): 6.10	SSI-042 inhibition (%): 47.80	SSI-043 inhibition (%): 98.90	SSI-044 inhibition (%): 189.00
SSI-045 inhibition (%): 76.70	SSI-046 inhibition (%): 92.70	SSI-047 inhibition (%): 59.50	SSI-048 inhibition (%): 61.00
SSI-049 inhibition (%): 44.20	SSI-050 inhibition (%): 100.90	SSI-051 inhibition (%): 103.80	SSI-052 inhibition (%): 83.90
SSI-053 inhibition (%): 83.00	SSI-054 inhibition (%): 71.90	SSI-055 inhibition (%): 68.50	SSI-056 inhibition (%): 61.40
SSI-057 inhibition (%): 55.50	SSI-058 inhibition (%): 1.50	SSI-059 inhibition (%): 75.40	SSI-060 inhibition (%): 47.20

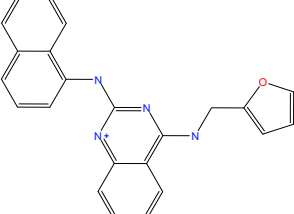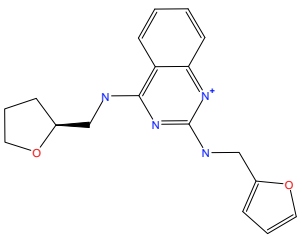|			
SSI-061 inhibition (%): 57.90	SSI-062 inhibition (%): 10.30	SSI-063 inhibition (%): 13.80	SSI-064 inhibition (%): 56.10
SSI-065 inhibition (%): 69.50	SSI-066 inhibition (%): 69.40	SSI-067 inhibition (%): 68.20	SSI-068 inhibition (%): 74.30
SSI-069 inhibition (%): 80.70	SSI-070 inhibition (%): 77.70	SSI-071 inhibition (%): 61.30	SSI-072 inhibition (%): 108.00
SSI-073 inhibition (%): 89.80	SSI-074 inhibition (%): 76.60	SSI-075 inhibition (%): 96.70	SSI-076 inhibition (%): 100.70
SSI-077 inhibition (%): 55.20	SSI-078 inhibition (%): 68.10	SSI-079 inhibition (%): 68.00	SSI-080 inhibition (%): 94.30

SSI-081 inhibition (%): 75.90	SSI-082 inhibition (%): 72.40	SSI-083 inhibition (%): 75.40	SSI-084 inhibition (%): 111.60
SSI-085 inhibition (%): 58.70	SSI-086 inhibition (%): 84.00	SSI-087 inhibition (%): 82.70	SSI-088 inhibition (%): 107.90
SSI-089 inhibition (%): 79.60	SSI-090 inhibition (%): 68.90	SSI-091 inhibition (%): 6.10	SSI-092 inhibition (%): 104.70
SSI-093 inhibition (%): 154.70	SSI-094 inhibition (%): 68.60	SSI-095 inhibition (%): 46.80	SSI-096 inhibition (%): 0.50
SSI-097 inhibition (%): 58.70	SSI-098 inhibition (%): 98.80	SSI-099 inhibition (%): 104.60	SSI-100 inhibition (%): 77.30

SSI-101 inhibition (%): 63.40	SSI-102 inhibition (%): 60.00	SSI-103 inhibition (%): 137.10	SSI-104 inhibition (%): 1.00
SSI-105 inhibition (%): 139.90	SSI-106 inhibition (%): 86.50	SSI-107 inhibition (%): 119.40	SSI-108 inhibition (%): 177.80
SSI-109 inhibition (%): 119.20	SSI-110 inhibition (%): 237.70	SSI-111 inhibition (%): 241.10	SSI-112 inhibition (%): 106.00
SSI-113 inhibition (%): 65.80	SSI-114 inhibition (%): 93.50	SSI-115 inhibition (%): 139.40	SSI-116 inhibition (%): 210.80
SSI-117 inhibition (%): 131.20	SSI-118 inhibition (%): 112.90	SSI-119 inhibition (%): 92.10	SSI-120 inhibition (%): 69.20

SSI-121 inhibition (%): 159.10	SSI-122 inhibition (%): 151.00	SSI-123 inhibition (%): 102.40	SSI-124 inhibition (%): 99.00
SSI-125 inhibition (%): 121.80	SSI-126 inhibition (%): 75.00	SSI-127 inhibition (%): 484.20	SSI-128 inhibition (%): 547.10
SSI-129 inhibition (%): 391.30	SSI-130 inhibition (%): 185.00	SSI-131 inhibition (%): 149.00	SSI-132 inhibition (%): 190.40
SSI-133 inhibition (%): 338.00	SSI-134 inhibition (%): 223.70	SSI-135 inhibition (%): 153.30	SSI-136 inhibition (%): 165.00
SSI-137 inhibition (%): 235.60	SSI-138 inhibition (%): 254.80	SSI-139 inhibition (%): 76.90	SSI-140 inhibition (%): 98.60
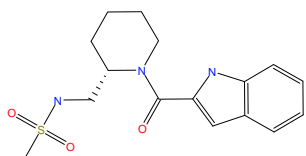
SSI-141
inhibition (%): 180.70
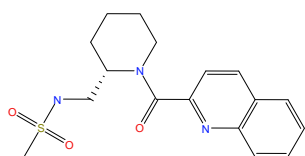
SSI-142
inhibition (%): 141.20
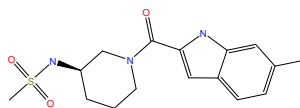
SSI-143
inhibition (%): 125.30

References:

1. F. K. Pettit, E. Bare, A. Tsai and J. U. Bowie, *Journal of molecular biology*, 2007, **369**, 863-879.
2. N. A. Baker, D. Sept, S. Joseph, M. J. Holst and J. A. McCammon, *Proceedings of the National Academy of Sciences of the United States of America*, 2001, **98**, 10037-10041.
3. P. C. Hawkins and A. Nicholls, *Journal of chemical information and modeling*, 2012, **52**, 2919-2936.
4. P. C. Hawkins, A. G. Skillman, G. L. Warren, B. A. Ellingson and M. T. Stahl, *Journal of chemical information and modeling*, 2010, **50**, 572-584.
5. B. O. Villoutreix, N. Renault, D. Lagorce, O. Sperandio, M. Montes and M. A. Miteva, *Current protein & peptide science*, 2007, **8**, 381-411.
6. G. Jones, P. Willett and R. C. Glen, *Journal of computer-aided molecular design*, 1995, **9**, 532-549.
7. H. Gohlke, M. Hendlich and G. Klebe, *Journal of molecular biology*, 2000, **295**, 337-356.
8. G. Neudert and G. Klebe, *Journal of chemical information and modeling*, 2011, **51**, 2731-2745.
9. A. Voet, F. Berenger and K. Y. J. Zhang, *PloS one*, 2013, **8**, e75762.
10. Y. Uchimura, M. Nakao and H. Saitoh, *FEBS letters*, 2004, **564**, 85-90.
11. N. Rouleau, J. Wang, L. Karras, E. Andrews, M. Bielefeld-Sevigny and Y. Chen, *Analytical biochemistry*, 2008, **375**, 364-366.
12. T. Kigawa, T. Yabuki and S. Yokoyama, *Tanpakushitsu kakusan koso. Protein, nucleic acid, enzyme*, 1999, **44**, 598-605.
13. T. Matsuda, S. Koshiba, N. Tochio, E. Seki, N. Iwasaki, T. Yabuki, M. Inoue, S. Yokoyama and T. Kigawa, *Journal of biomolecular NMR*, 2007, **37**, 225-229.
14. J. Yokoyama, T. Matsuda, S. Koshiba, N. Tochio and T. Kigawa, *Analytical biochemistry*, 2011, **411**, 223-229.
15. F. Delaglio, S. Grzesiek, G. W. Vuister, G. Zhu, J. Pfeifer and A. Bax, *Journal of biomolecular NMR*, 1995, **6**, 277-293.
16. N. Kobayashi, J. Iwahara, S. Koshiba, T. Tomizawa, N. Tochio, P. Guntert, T. Kigawa and S. Yokoyama, *Journal of biomolecular NMR*, 2007, **39**, 31-52.
17. B. A. Johnson, *Methods Mol Biol*, 2004, **278**, 313-352.